Science and Technology Facilities Council

ITRF Project

LhARA Laser-hybrid Accelerator for Radiobiological Applications

Document Filename: 1272-pa1-pm-rpt-0008-v0.2 milestones 6 & 7 report

29th February 2024

DRAFT

ITRF & LhARA Reporting M6 & M7

Milestone 6 *Preliminary design of LhARA MA RF cavity, FFA magnet, diagnostic system, control & feedback systems*

Milestone 7 *Preliminary design study of LhARA Building concept design, bulk shielding assessment, mechanical systems integration support concepts, vacuum concepts, power consumption & cooling requirements*

Change record

Version	Changes to document	Author	Date
0.1	template only	C. Hill	13/02/24
0.2	First draft	See report	29/02/24
0.3	Added section on RF	Ajit Kurup	19/03/24
0.4	Added section on FFA magnet	Ta-Jen Kuo	04/04/24
0.5	Added diagnostics section from Jaroslaw Pasternak	Ajit Kurup	23/04/24

UKRI-STFC internal store: here

ITRF SharePoint store: here

1. MA RF Cavity – *Ajit Kurup*

The machine parameters related to the cavity are given in Table 1 . The main parameters are the frequency range of 2.89 – 6.48 MHz and the voltage requirement of 4kV. Two technology choices are being considered for the LhARA FFA cavity: ferrite loaded; and magnetic alloy loaded.

Parameter	Value
Proton RF frequency	2.89 – 6.48 MHz
Voltage per cavity	4 kV
Bunch intensity	10^8 protons/bunch
Harmonic number	1
Horizontal aperture	65 – 85 cm
Vertical aperture	Around 7 cm

Table 1: RF parameters

The RF cavity for the FETS FFA, which has similar requirements to the LhARA cavity, is being developed by the ISIS synchrotron RF group. Similarly, both ferrite cores and magnetic alloy cores are being considered and measurements of material properties of prototype cores are in progress.

Ferrite-loaded cavity

Figure 1 is a schematic diagram of a ferrite loaded cavity. Details of the analysis of this can be found in [1]. The bias current I_{gen} induces a magnetic field in the ferrite discs and is used to modulate μ'_p which allows the resonant frequency to be swept over the required range.

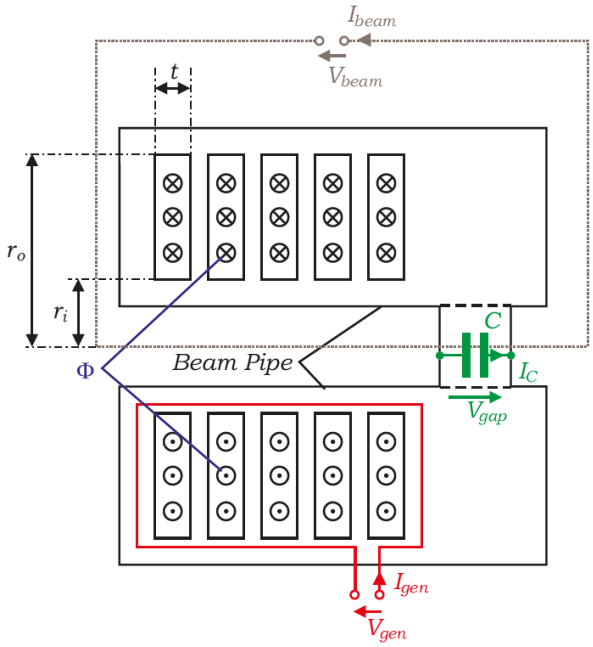

Figure 1: Simplified schematic of a ferrite cavity [1].

$$R_p = \omega \frac{N t \mu'_p Q}{2\pi} \, ln\frac{r_o}{r_i} = N t \mu'_p Q f \, ln\frac{r_o}{r_i}$$

Equation 1: Shunt impedance of a ferrite cavity. See [1] for derivation.

The shunt impedance is given by Equation 1, see [1] for the derivation. This consists of a term purely dependent on geometry $Nt \ln\frac{r_o}{r_i}$ and a term given by the characteristics of the material $\mu'_p Q f$. The material term is often quoted by manufacturers and is dependent on frequency, see Figure 2 for examples of $\mu'_p Q f$ for different materials. The cavity design is dependent on measuring $\mu'_p Q f$ over the required frequency range and under the high-power conditions that the cavity will be operated under as these will have a major impact on the performance of the cavity.

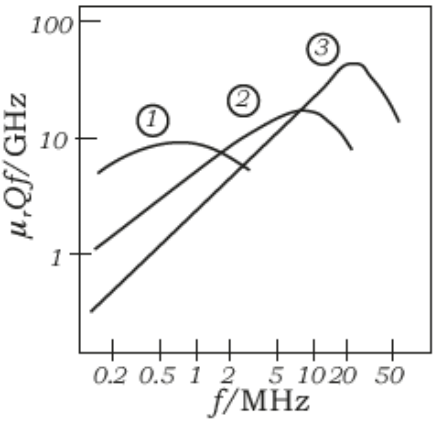

Figure 2: $\mu_r Qf$ product versus frequency for three different types of ferrite material (1: Ferroxcube 4A, 2: Ferrox-cube 4C, 3: Ferroxcube 4E). Taken from [1]

The other major components required for a ferrite cavity are: bias current power supply; RF power amplifier chain; and a low-level RF control system. The bias power supply must be capable of ramping the required current, within the period for one acceleration cycle, to vary μ_p' and thus sweep the resonant frequency over the required range.

Magnetic alloy-loaded cavity

Magnetic alloy (MA) loaded cavities are similar to ferrite cavities in that they utilise an inductive core to give a relatively low resonant frequency. In the case of the MA core cavity, the permeability and the saturation magnetic field are much higher than ferrite cores so there is no need to use a bias supply to sweep the resonant frequency as the cavity has such a large bandwidth. This also means the power amplifier system and the low-level RF system are much simpler. However, since the cavity has a low Q-value, the power dissipated in the cores will be higher and this would have an impact on the running cost of the cavity. The core is made from a metallic ribbon that has an insulation layer to provide electrical isolation between adjacent layers. The ribbon is then wound into the shape needed for the aperture of the cavity. The core then undergoes either an annealing or a nano-crystallisation process.
Figure 3 shows a schematic of the MA core cavity for the FETS FFA and Figure 4 is a photo of a prototype core purchased by the ISIS synchrotron group to measure the $\mu_p' Qf$ of the material.

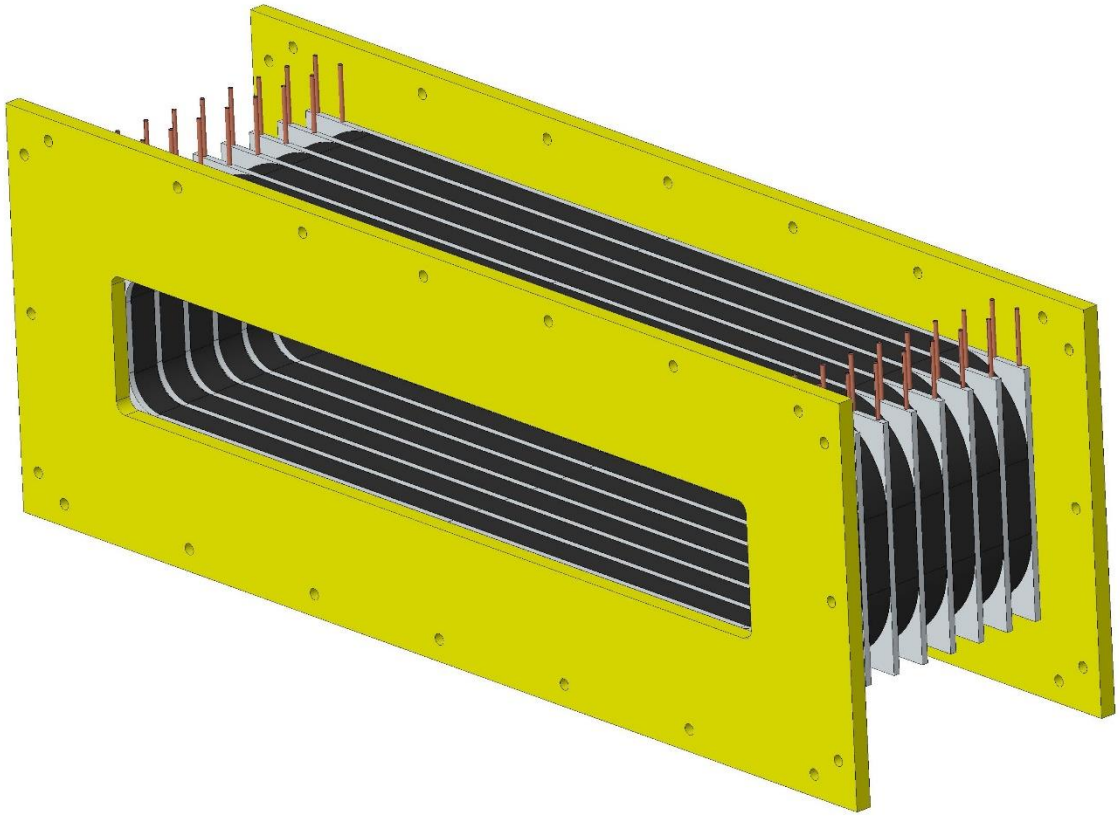

Figure 3: Schematic of the magnetic alloy core cavity.

Figure 4: A prototype core to be tested for the FETS FFA RF cavity

Figure 5 shows the $\mu_p' Qf$ as a function of the RF magnetic field. As can be seen, the MA cores do not suffer from saturation effects like the ferrite cores.

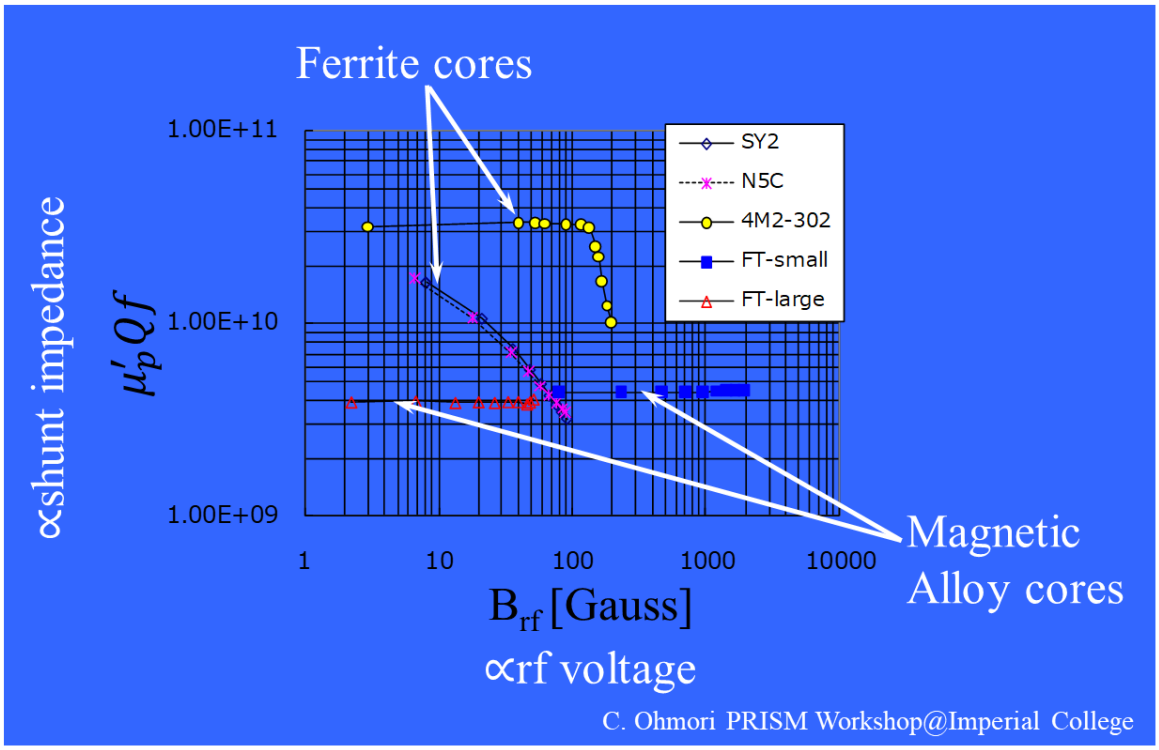

Figure 5: $\mu'_p Qf$ versus RF magnetic field for ferrite and MA cores

Plans

The main goal is to evaluate the viability of both technologies for the requirements of the LHARA FFA. This mainly requires measurements of the material parameters. Such measurements of the material characteristics are being done for the FETS FFA and these results can be used to evaluate the pros and cons of both technology choices for the LhARA FFA. The ferrite loaded option requires the magnetic field in the cores stay below the saturation limit. Although this can be mitigated by adding more cores this will also increase the length of the cavity, which must fit within the space available between the FFA magnets. Cost considerations for choosing one technology would include, the cost and complexity of the bias power supply, the high-power RF system and the low-level RF system versus the estimated running cost of the MA cavity. The MA cores are more complex to manufacture than the ferrite cores and may require a specific QA procedure to ensure the cores will maintain their performance over the operational period of the facility. Though since the voltage requirements for LhARA are very modest compared to other facilities that have built and operated MA core cavities, the mechanical forces that could deform the core when operating at high power is not expected to be an issue.

2. FFA Magnet – *Ta-Jen Kuo*

2.1 PRELIMINARY DESIGN

The parameters of the FFA magnet are given in Table 2. The FFA ring consists of ten symmetric cells, each containing a single combined-function spiral magnet.

Parameter	Value
Number of cells	10
k range	4.37-5.55
dk/k (%)	< 1
Spiral angle (Degrees)	48.7
r_0(m)	3.477
B_0 (T)	1.405
Packing Factor	0.34

Table 2: Parameters of the FFA magnet

The field index k is defined as $k = \frac{r}{B_z}\frac{\partial B_z}{\partial r}$ where B_z is the vertical magnetic field. The FFA is required to deliver beams over a range of energy; each requiring a particular k index for the ring magnets. In an FFA magnet, the integrated magnetic field on the median plane should follow the scaling law: $BL = BL_0 \left(\frac{r}{r_0}\right)^{k+1}$ $where\ BL = r \int B_z\, d\theta$, $BL_0 = r_0\, B_0\, \Delta\theta$ and $\Delta\theta$ is the opening angle of the magnet.

The scaling magnetic field is generated by having distributed conductors, a main coil and 18 trim coils. A main coil wrapped around a flat pole generates the constant dipole field. The trim coils cross the pole face and return towards the outer radii of the pole. Powered with different currents, they generate the gradient of the B field. The details of the trim coils and a calculation of the total power required for the currents can be found in Table 3.

The configuration of the conductors can be found in figure 6. The trim coils are wrapped in two different vertical layers, with an 0.5 offset between the two layers; this has been shown to improve the field quality by studies down on the FETS-FFA magnet with similar properties [2]. The main coil is labelled as 0 and has a dimension of 75mm x 95 mm, whereas the trim coils labelled from 1-18 with as dimension of 10mm x 92.5mm.

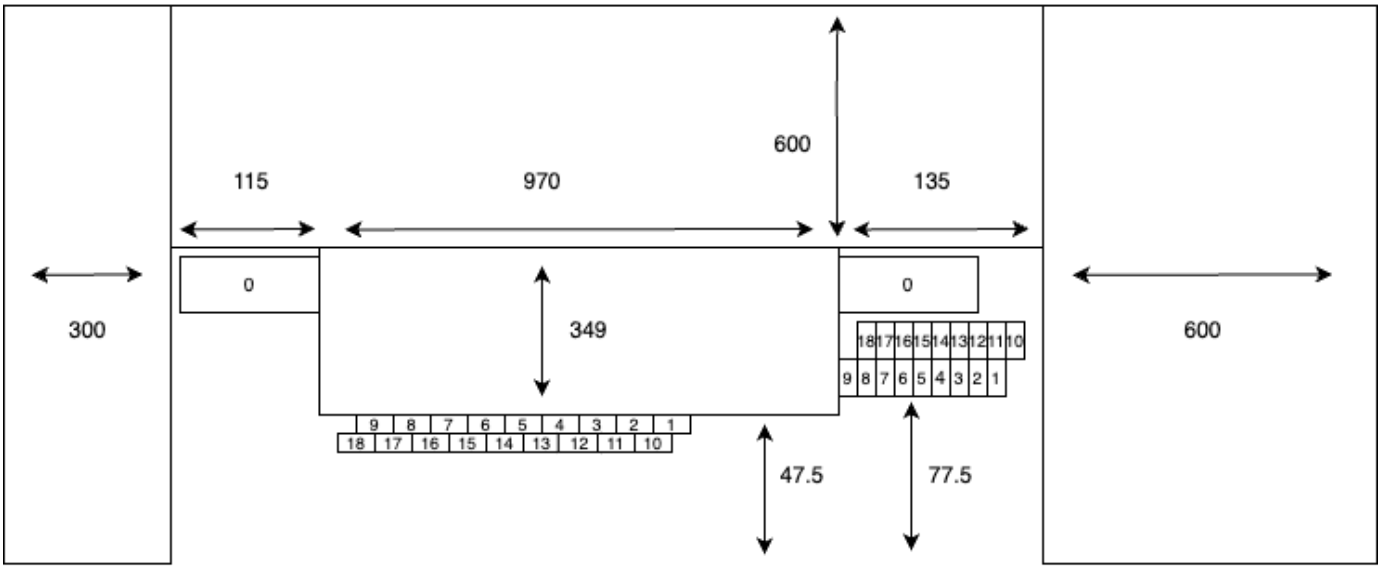

Figure 6: Schematic diagram of the cross section of the FFA magnet. The dimensions of the magnet are labelled in millimetres and the conductors are labelled from 0-18.

2.2 3D model

A 3D model was created in OPERA-3D with the specifications given above, the model was successfully computed with a target k index of 5.33. The field quality along the midplane can be found in figure 9.

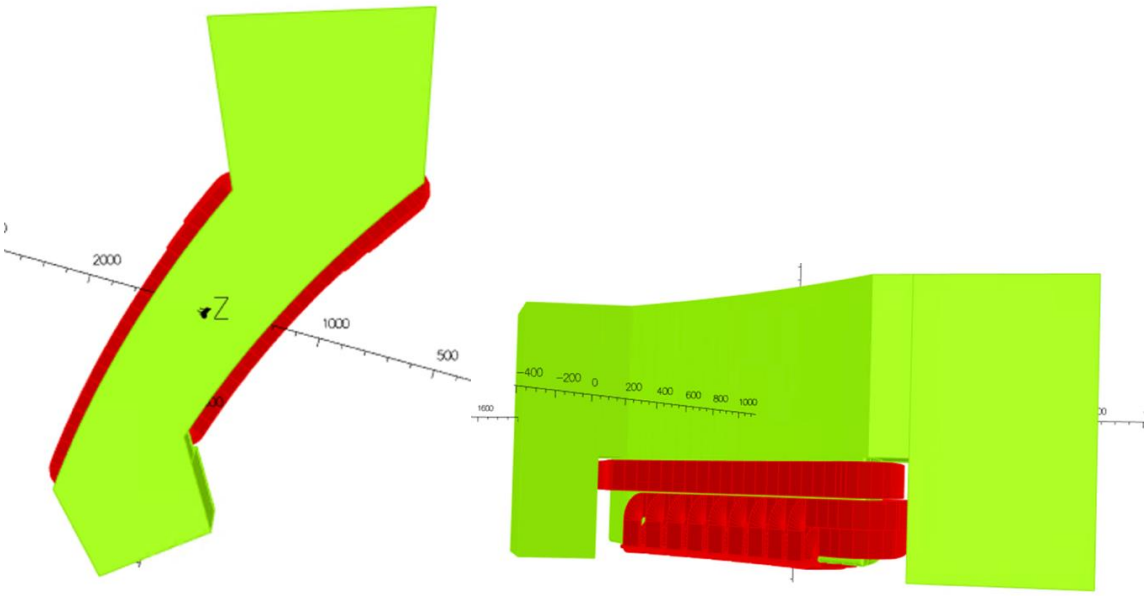

Figure 7: 3D model of the FFA magnet modelled in OPERA-3D, only the top half of the magnet is shown. The conductors are shown in red with the iron in green. (Left) Top view (Right) Side view

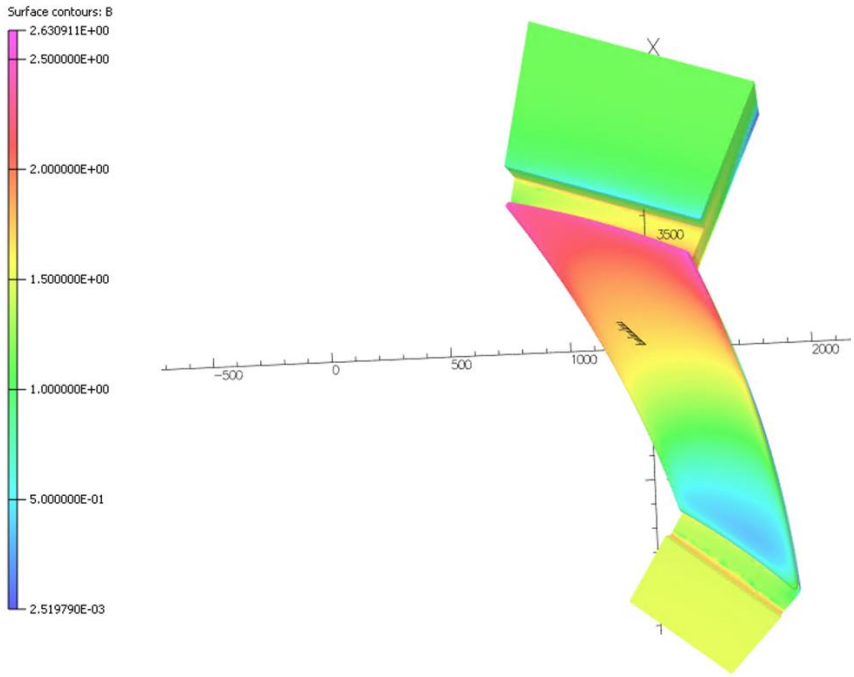

Figure 8: Saturation of the pole face of the magnet in OPERA-3D. It can be seen to reach up to 2.6T at higher radii which is far into the saturation region.

Coil Number	Length (m)	Ampere Turn	Power (W)
0	4.48	14227	2480
1	2.36	6220	2370
2	2.57	4220	1190
3	2.78	3416	841
4	2.98	2834	622
5	3.20	2411	483
6	3.41	2065	377
7	3.61	1774	295
8	3.82	1495	222
9	4.02	1183	146

10	2.75	6220	2760
11	2.96	4220	1370
12	3.16	3416	958
13	3.37	2834	703
14	3.58	2411	540
15	3.79	2065	420
16	4.00	1774	327
17	4.20	1495	244
18	4.41	1183	160
		Total Power (W)	16,500

Table 3: The coil number corresponds to the ones labelled in Figure 6. The total power calculated was for a half of the magnet.

2.3 Results

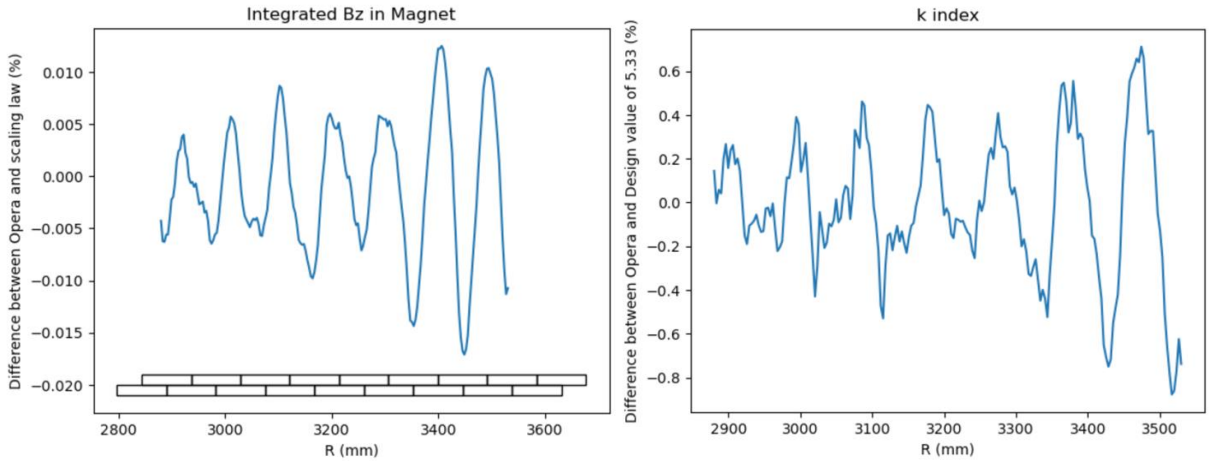

Figure 9: Field quality obtained from the OPERA-3D model. (Left) Difference between the integrated Bz in the model compared to the scaling law. The positions of the trim coils are shown at the bottom of the graph to compare the oscillation in the field quality to the structure of the trim coils. (Right) Difference between the k index calculated from the B field obtained from the model compared to the designed value of 5.33.

The field quality obtained from the OPERA-3D model can be found in Figure 9. The error of the k index falls within +/- one percent which was the requirement from Table 2. Field clamps will be added to either side of the magnet in the future to meet the scaling conditions: fringe field extent scaling with radius and the spiral angle of the magnetic field being constant.

3. Diagnostic System – *Jaroslaw Pasternak*

3.1 Introduction

The LhARA facility will require several diagnostic systems in order to deliver the quality beam for radiobiology experiments. The choice of diagnostics depends on the beam properties and LhARA will have a very specific beam due to the use of the laser source. The beam created at the target will have large peak current, very low emittance, high brightness, and very short bunch length, but low average current. While propagating downstream the beam-line beam will undergo emittance growth and some beam loss is expected. The bunch length will also increase from almost zero to the ~ns range in Stage 1 and tens of ns in Stage 2. In this section the diagnostics for commissioning and operation of the accelerator facility is discussed and the dedicated diagnostics systems for beam dose and quality measurements at the end-stations are not covered.

3.2 Stage 1, Injection line to FFA and High Energy Beam Transfer (HEBT)

In order to commission and later operate LhARA at Stage 1, the key parameters to be measured are beam size, beam position and beam current. The beam size and beam position can be measured with scintillating screens or Secondary Electron Emission (SEM) grids, which would need to be retractable. The beam current can be measured non-destructively with Wall Current Monitors (WCMs), most likely passive ones due to the shortness of the bunch.

Similar set of devices will be needed in the injection line to the FFA and in the Stage 2 after extracting from the FFA, in HEBT.

Precise measurement of bunch length may be challenging in the Stage 1 due to a very short bunch length from the laser source and will require dedicated study. In Stage 2 after extraction from the FFA it may be possible to use WCMs as the bunch length will be longer.

Another useful quantity to measure will be beam loss, which can be performed with beam loss monitors based on plastic scintillators, for example. Those monitors will be placed in the vicinity of the beam pipe in the areas where beam loss is expected.

3.3 FFA

FFA will have special requirements due to an un-even size of the vacuum chamber, with very large horizontal dimension and relatively small vertical one, see Table 1 for estimates of the values. The key measurements to commission and operate FFA ring will be the beam trajectory (the turn-by-turn position measurement), measurement of betatron tunes and the beam current. The beam trajectory will be measured with capacitive pick-ups. The single pick-up device to measure both horizontal and vertical trajectory simultaneously is in development for FETS-FFA at RAL [3].

The tune measurement can use the same capacitive pick-up, however it standard realisation will require beam perturbation. This beam perturbation can be performed by injection and extraction kickers, but only in the vicinity of injection and extraction orbits as kickers will only cover those areas. In addition, this will only allow for the horizontal tune measurement, as both injection and extraction are planned to be in the horizontal plane. FFA requirement is to be able to measure tune for all stable orbits from injection to extraction in both transverse planes.

In order to measure horizontal tune on any orbit the RF knock-out method was developed [4]. It explores the fact that horizontal dispersion exists in the machine, so if beam receives a short acceleration burst from the RF cavity, it will start to oscillate. The vertical measurements will require a vertical exciter, either magnetic or electric.

There is also a possibility to investigate the so-called Base-Band Q (BBQ) Measurement with Direct Diode Detection [5], which allows to measure tunes without any external excitation, however this method was never used in FFAs up to date.

The current measurement will be performed using WCM with dimensions required by the FFA. This device should also allow to measure bunch length and be used to measure RF phase.

Beam profile measurement could be performed using wire scanner.

Beam loss can be measured in similar way as in Stage 1.

3.4 Status and future plans

All diagnostic devices discussed in the context of Stage 1 are based on established technology with the exception for the bunch length measurement which requires further study. The FFA diagnostics was already demonstrated at KURNS and its development is now progressing in the context of FETS-FFA. LhARA project should develop further collaboration with FETS-FFA project in the domain of diagnostics.

The locations of the beam profile monitors and WCMs for Stage 1 were established, and work is under way for the injection line. Locations for diagnostics in FFA and for HEBT will be studied next.

[3] D. Posthuma de Boer, E. Yamakawa, private communication
[4] https://ffag.pp.rl.ac.uk/FFAG/FFAG09J_HP/slides/Takahoko-FFAG09j.pdf
[5] http://mgasior.web.cern.ch/pro/bbq/index.html

4. Control and Feedback Systems – *Graham Cox (STFC Daresbury)*

4.1 Introduction

The control system plays a central role in all accelerator facilities. The LhARA control system will be a facility wide monitoring and control system integrating all parts of the LhARA facility. The control system will extend from the interface of the equipment being controlled in the technical sub-systems through to the operator, engineering expert or physicist. It will include all hardware and software between these bounds including computer systems, networking, hardware interfaces, programmable logic controllers (PLCs) and fieldbuses.
The Personnel Safety System (PSS) will be interfaced to, and monitored by, the LhARA control system. A separate event synchronisation system will be implemented as part of the control system to ensure synchronisation of technical sub-systems and critical control operations and will also provide a common high resolution time-stamping and/or pulse numbering capability.
The LhARA control system will benefit from existing control system equipment standards and knowledge gained from recently implemented ASTeC Radiation Test Facilities e.g. CLARA. Consideration has been made for where technology has progressed e.g. new, more appropriate fieldbuses or protocols will be implemented.

4.2 Architecture

The LhARA control system will be implemented using the EPICS software toolkit. EPICS is a proven software toolkit with well-defined interfaces at both the client and server and will enable fast integration and development. Due to its collaborative nature, using EPICS enables LhARA to take advantage of work done at other laboratories. EPICS has been successfully applied on previous projects at Daresbury including the ALICE, EMMA, VELA and CLARA facilities and on many accelerator projects worldwide. For these previous Daresbury projects extensive use has been made of EPICS version 3 and more recently EPICS version 7. For LhARA it will be possible to deploy version 7 and utilise the advanced features exposed via the pvAccess protocol including manipulation and transport of structured data over the network.
The various components of the control system will be connected to a high speed Ethernet local area network. This will consist of several class C subnets connected to the main site network. Access will be provided to the control system data via EPICS gateway systems running access security.

The hardware interface layer of the control system will provide the connection to the underlying sub-systems. This will consist of a modular hardware solution of commercial rack mount PCs and embedded systems running the Linux operating system, real-time where required, connected to a range of I/O types directly or via selected fieldbuses.
Application software will be installed on central file servers to ensure consistent operation from any console on the control system network. The control system will be implemented in such a way that it can be incrementally expanded and upgraded as the project proceeds. The control system must be able to be extended to new hardware and software technology during the project phases and later. A number of EPICS client interfaces will be supported for controls and physics application development in high-level languages. This is likely to include both Channel Access and pvAccess interfaces for languages such as C#/VB via .NET, Matlab, Mathematica and Python.

4.3 Controls Hardware

The network hardware and commercial PC hardware of the LhARA control system will use standards defined by the STFC Digital Infrastructure department.
As far as possible controls hardware used on recent ASTeC Radiation Test Facilities should be preferred to take advantage of existing expertise and proven hardware standards.
This hardware includes:
• *Industrial rack mount PC systems running a Linux operating system, with potential for a real-time kernel, as required:* Existing EPICS support is available for interfacing many I/O types including analogue, digital and serial (RS232/422/485) along with status/interlocking via Ethernet connected Programmable Logic Controllers.
• *Omron NJ series PLCs:* Status and interlock systems for digital control and machine protection of accelerator hardware and sub-systems. As a replacement for Omron CJ series PLCs deployed on previous ASTeC RTFs, the NJ PLCs will either be integrated directly into the EPICS control system utilising the CIP protocol, or indirectly via a data aggregation tool with EPICS integration via OPC-UA or similar. This will allow PLC data tags to be directly mapped to EPICS process variables and/or to pvAccess structured data types.
• *Motion control systems:* Fieldbus based systems with remote I/O via EtherCAT. In common with CLARA and building on this experience, these will comprise of Beckhoff TwinCAT real-time controllers with EtherCAT connected motion control and I/O modules. These controllers interface with the EPICS control system via Modbus TCP.
Any specialist control requirements would be solved by using dedicated real-time controllers (for example embedded industrial hardware or FPGA based). Examples of such systems could include geographically isolated devices or systems that require the computing speed of a dedicated CPU. Any dedicated controllers would be integrated into the EPICS environment and software build processes.
Due to the pulsed nature of the facility dedicated real-time systems will be required to satisfy these requirements. Likely applications include data acquisition for beam diagnostic measurements or RF system measurements. For previous ASTeC RTF control systems VMEbus processors and FPGA based I/O carriers have been utilised. For LhARA it is expected the modular, open standard, MicroTCA will be adopted as a replacement for VMEbus. Options for embedded MicroTCA controllers and FPGA carriers will be evaluated further in the Technical Design phase.

4.4 Virtualisation

Virtualisation technology will be utilised both in the server infrastructure layer and, where appropriate, in the EPICS input/output controllers. This will increase flexibility, scalability,

reliability and efficiency of the control system by abstracting hardware specifics from the controls software.

4.5 Timing and Synchronisation System

One of the principle challenges with a network distributed control system is the synchronisation and accurate time-stamping or pulse numbering of events spread across several physically and logically separated systems. An example of this is the simultaneous measurement of beam diagnostic information along an entire beam transport system. This operation will typically involve collecting beam-synchronous data simultaneously from a number of front-end server systems.
Commercially available synchronisation hardware, as used on CLARA (Micro-Research Finland), is available for a number of platforms and provides timing outputs for LhARA applications.
It will be important to ensure that the master clock used by the timing system is locked to the RF and laser systems of LhARA. GPS atomic clock synchronisation will be used to distribute accurate time via the timing system and can also be used to discipline the RF master oscillator.

4.6 Interlock Systems

The control system will provide a comprehensive interlock and machine protection system ranging from the enforcement of sensible operating limits right through to the protection of the facility against potentially dangerous operating conditions.

High Integrity

If and where required, this will be used to provide high-speed and fail-safe local protection in situations where serious damage to equipment is likely to occur. Embedded micro-controllers could be used for this purpose.

Routine

This level of protection is intended to prevent minor damage to individual machine components or sub-systems. An Omron PLC based interlock system based on experience of other facilities will be used for this purpose.
Both interlock systems will operate independently of EPICS with monitoring and control requests marshalled to the interlock systems via EPICS for processing via internally programmed logic. In addition, but not described here, there will also be local systems that supervise individual components such as RF structures.

Personnel Safety System

This section does not cover details of the protection of personnel from facility hazards. In terms of logic implementation, the PSS would be implemented using Omron safety controllers. The NX controllers make use of Ethernet based safety protocols and are more suited to a new facility, easing installation and enabling greater scalability and flexibility. Full monitoring of the PSS will be provided through the control system.

4.7 Feedback Systems

Digital feedback will be required in a number of places on LhARA. The primary requirements include closed loop control of amplitude/phase in RF systems and water cooling for high-power RF infrastructure and accelerating cavities.
For slow feedback control e.g. water temperature stabilisation, this shall either be implemented in the commercially supplied system, or within the control system via PLC or

EPICS PID control. In the case of commercial systems, they should ideally support integration into the control system to allow remote monitoring and control of the process. For faster, lower latency feedback control, this will be integrated directly into the control system. In the case of RF amplitude/phase control, this shall be either by embedding the control directly into the FPGA of the LLRF controller, or by dedicated software directly on the CPU of the LLRF controller. Options for embedded feedback control will be evaluated further in the Technical Design phase.

4.8 High-level Application Software

For operation of the LhARA facility high-level physics applications are required that will communicate with the facility via the control system. To abstract away the detailed implementation of devices in the control system, a mid-level interface is required. This allows operators and physicists to interact with sub-systems and devices in a consistent, structured and well-defined way. Options developed and used previously include common C++/Python middle-level-interface to the control system, CATAP: 'Controls Abstraction To Accelerator Physics'. Also pvAccess interface using EPICS version 7 to represent sub-systems and devices as consistent, structured data for direct consumption by high-level application software.

5. LhARA Building Concept Design – *Clive Hill (STFC Daresbury)*

Referring to document 1272-pa1-pm-rpt-0007-v1.0-twelve-month-design-review-report (page 54) the building concept design is well described and has not changed significantly since the report was published.

Work is progressing in the region of the FFA ring and the building size requirements will need to be reviewed when the position and size of the ring has been determined.

6. Bulk Shielding Assessment- *James Bebbington (STFC Daresbury)*

Consolidation of source terms

The output of a shielding assessment is entirely dependent on the source terms that are provided to the calculation.

A collaborative meeting held at Daresbury Laboratory on 1st November 2023 involving physicists from each institution, relevant STFC staff and an external shielding assessor focussed the attention of the various stakeholders on the issue of the source description. This proved to be instrumental in explaining what source term format was required to enable utilisation in shielding calculations and laid the foundations for the functional source term data sheet currently being used to perform the bulk shielding assessment.

The sheet consists of a schematic of the facility, displaying each significant source; this is each location where a substantial proportion of the proton beam is lost, such as the collimators, the shutters and the beam dumps. The beam loss statistics for each source in each mode are outlined in the table below (grey shading denotes the termination of the beam), noting that for Modes 2 and 6, the beam either ends at the In-vitro or In-vivo station and not both simultaneously:

Location		Beam loss percentage (%)

	Source description	Mode 1	Mode 2	Mode 3	Mode 4	Mode 5	Mode 6
A0	Plasma source	98	98	98	98	98	98
A	Source nozzle	30	33	30	30	30	30
B	Collimator	25	25	25	25	25	25
C	Source shutter	0	0	100	0	0	0
D	In-vitro Stage 1 delivery (arc collimator)	25	0	0	25	0	0
E	In-vitro Stage 1 station	100	0		100	0	0
F	Injection line (Stage 1 shutter)	0	25		0	25	25
G	FFA acceleration		10			50	10
H	FFA extraction		10			10	10
I	FFA beam dump		0			100	0
J	FFA shutter		0			0	0
K	In-vitro Stage 2 delivery		0 or 25				0 or 25
L	In-vitro Stage 2 station		0 or 100				0 or 100
M	Stage 2 shutter		0				0
N	In-vivo delivery		0 or 100				0 or 100

Additionally, the initial plasma source term has been simulated and all key parameters such as the beam energy distribution, divergence, initial proton/ion yield have been derived from this. Combining this plasma source with the loss points, each mode of operation has now been described in terms of which source points are engaged and what the particle loss rate is at that point. The source term also contains the operating schedule; the temporal parameters, such as the availability of the machine and the expected duration of "beam on" time and which fraction of this is attributed to each operational mode, which are necessary in understanding accumulated exposures and residual activation of components.

As of the date of this report, the final source description is only missing the initial electron component from the stripping of the protons at the very start of the process. Aside from that, the source term is complete for use in shielding calculations; the table below summarises the nominal, bounding source term for each stage of normal operation:

	Stage 1 operation		Stage 2 operation	
	Protons	**C6+ ions**	**Protons**	**C6+ ions**
Max beam energy (MeV)	15 MeV	48 MeV	127 MeV	400 MeV
Repetition rate (Hz)	100			
Particles required at delivery point (#/s)	1×10^{10}	1×10^{9}	1×10^{10}	1×10^{9}

Engagement of shielding assessors

The source term meeting held on 1st November 2023 introduced TÜV SÜD's dedicated shielding assessment team to the project, Nuclear Technologies. Expert guidance was provided in the initial meeting to ensure a suitable source term was described and their services are now fully engaged to provide the bulk shielding assessment to which this milestone relates.

A contract of work, split up into two phases was partially approved, with phase 1 work (shielding design basis and bulk shielding assessment) to be delivered next financial year (24/25) and phase 2 work (fault scenarios, material activation and residual dose rate assessment) to be delivered at a later date, as and when the necessary finances become available. It is worth noting that the anticipated availability and duty cycle of the facility may give rise to significant residual activation, which may overtake the external dose rates as the limiting factor in these radiation assessments.

As of the date of this report, the shielding design basis is at around 70 % completion; final edits and a quality assurance check are required. This is the key document that establishes the standards, source and material data, radiological design criteria and layout with approach to designation of areas which will be utilised for all facility radiation shielding calculations. This allows a consistent approach to all shielding calculations attributed to the facility, even between different shielding assessors and formalises any assumptions made in a transparent document. The designation of radiological areas methodology is also determined within the shielding design basis, containing projected area designations through the entirety of commissioning and normal operation phases.

From this shielding design basis, TÜV SÜD have now begun work on the bulk shielding assessment, with an estimated completion date in May/June 2024.

Next steps
In the upcoming financial year, the bulk shielding assessment for the facility will be delivered and interpreted, allowing it to feed into future operational and design decisions.

7. Mechanical Systems Integration Support Concepts - *Clive Hill (STFC Daresbury)*

7.1 Introduction

The support systems for accelerator devices are required to be stable, minimise effects due to vibration and include adjustment to facilitate accurate positioning of equipment. The support concepts adopted for LhARA have been developed and successfully implemented on other linear accelerator projects such as CLARA and ESS designed by the mechanical engineering group at STFC Daresbury.
The concept adopts a modular system which facilitates assembly and offline testing of accelerator equipment before installation into the accelerator hall enabling the most efficient use of time particularly during critical shutdown periods.

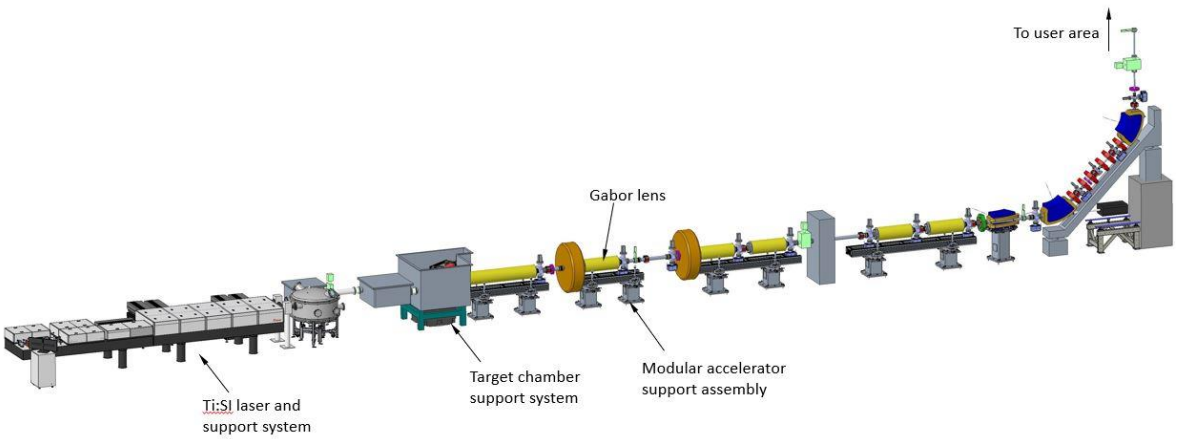

Fig 1

7.2 Ti:SI Laser Support System

It is envisaged that the Ti:Sapphire laser system will be procured and supplied by a specialist commercial company, the supports for this system will be included in the scope of design and procurement.

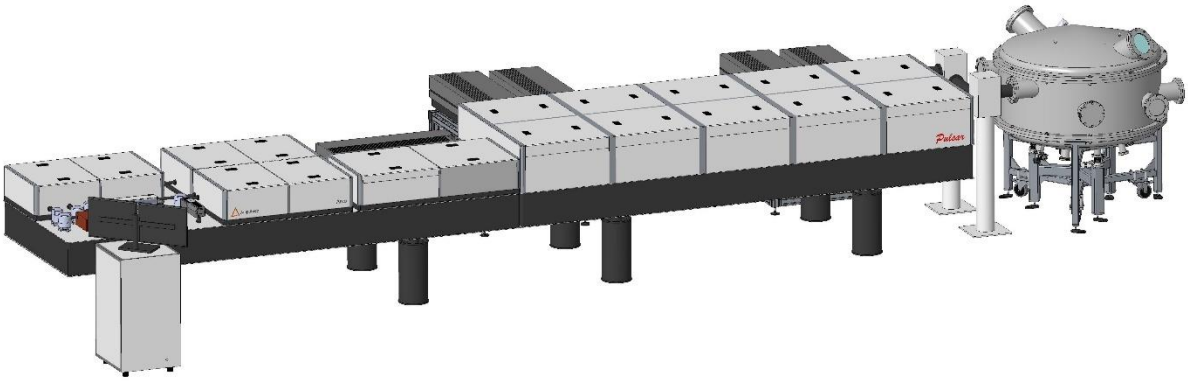

Fig 2

7.3 Laser Target Optics Support System

For optical support systems, such as the laser target chamber source, it is critical that the optical element supports are isolated from the vacuum chamber which will deflect during pump down. In figure 3 optics are shown mounted onto a baseplate which is isolated from the vacuum chamber with bellows and supported by a synthetic granite block for vibration damping. The vacuum chamber is supported by an independent frame with adjustments available in X , Y and Z.

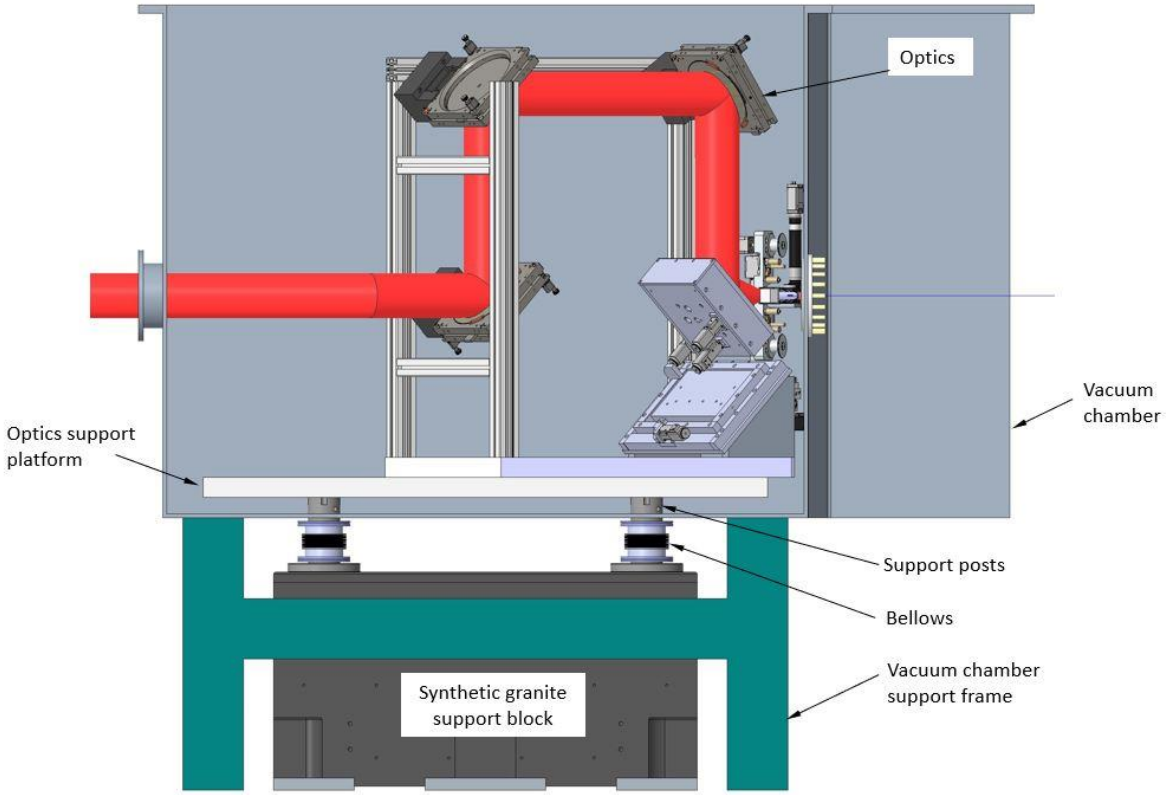

Fig 3

7.4 Accelerator Support Systems

Each modular support system includes two pedestals and an aluminium extruded beam as shown in figure 1. The support pedestals are fabricated mild steel consisting of a thick wall support tube with top and bottom plate. The beam assembly is constructed from rectangular aluminium extrusion commercially available which includes flat surfaces with tolerance specification, T-slot features for clamping accelerator equipment and ancillary equipment such as electrical and water services. The beam assembly is supported by the pedestals utilising a three point kinematic system allowing for adjustment in direction Y and also pitch, roll and yaw. Adjustment of the beam in directions X and Z is achieved by translation of a plate using screws.

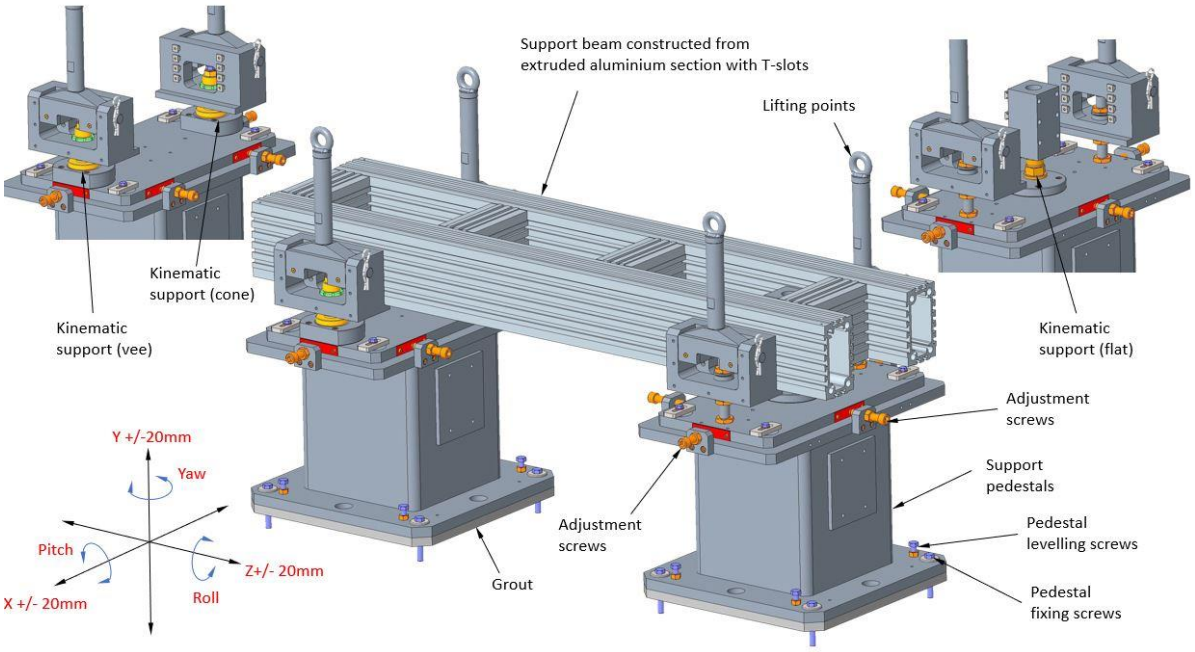

Fig 4

Accelerator equipment and devices that are assembled to the support beam have independent kinematic support and adjustment providing translation in X, Y and Z together with pitch roll and yaw. Figures 5 and 6 show examples of a quadrupole and corrector magnet assembled to a support beam. All accelerator devices will have features for inserting laser tracker survey fiducials to enable pre-alignment of each module.

The gabor lens support features have not been determined at this stage. However, it is envisaged that the proposed modular support beam system would be an appropriate concept as shown in Figure 7

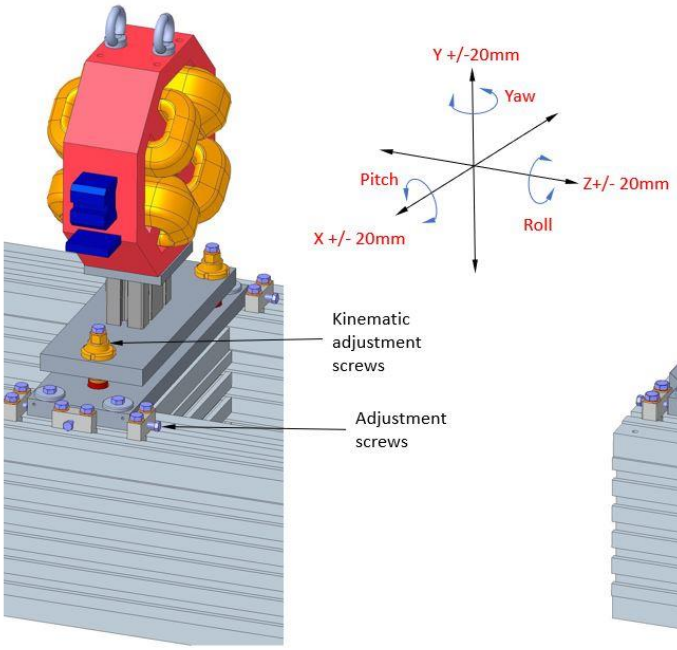

Fig 5

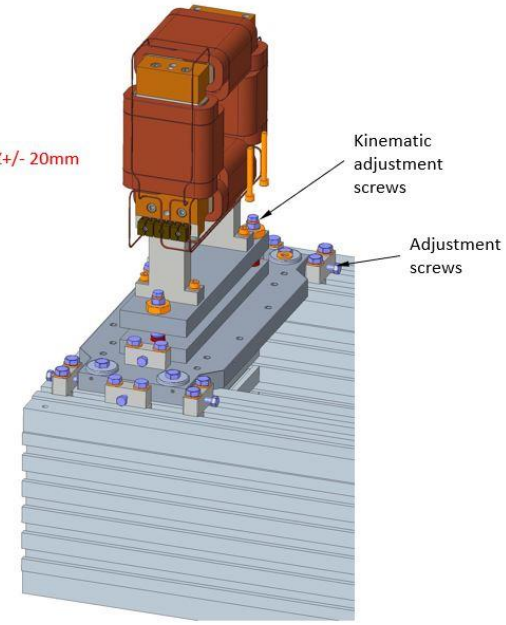

Fig 6

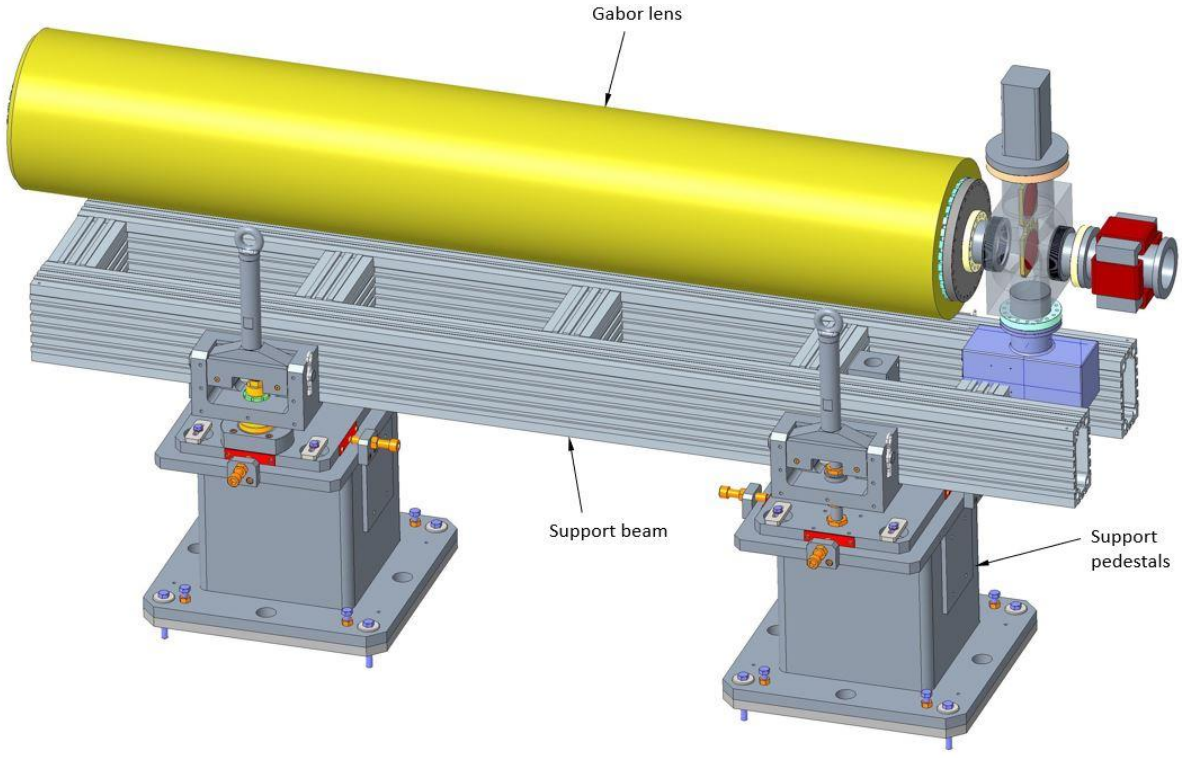

Fig 7

Building offline in a modular way also enables the installation of local services allowing for testing of systems such as vacuum integrity, magnet power and water cooling systems. Following offline testing the beam assembly module can be transported to the accelerator hall using a lifting beam and attachments. The support pedestals are installed with the bottom plate set 25mm above the floor and after levelling are secured with bolts and a high strength grout is applied in the gap under the pedestal plate. The pedestals are filled with dry sand to act as a vibration damper and minimise any effects on the accelerator devices. The aluminium

beam assembly is located using the three point kinematic support system and secured with fasteners.

Alignment of the beam assembly is achieved by using the adjustment features described above and with a laser tacker which accurately reads back the position of fiducials placed into holes in the corners of the beam assembly.

For accelerator equipment required for transporting the beam vertically to the user areas it is envisaged that the same modular system can be implemented. A concrete block can be used to elevate the support pedestal at one end as shown in Fig 8.

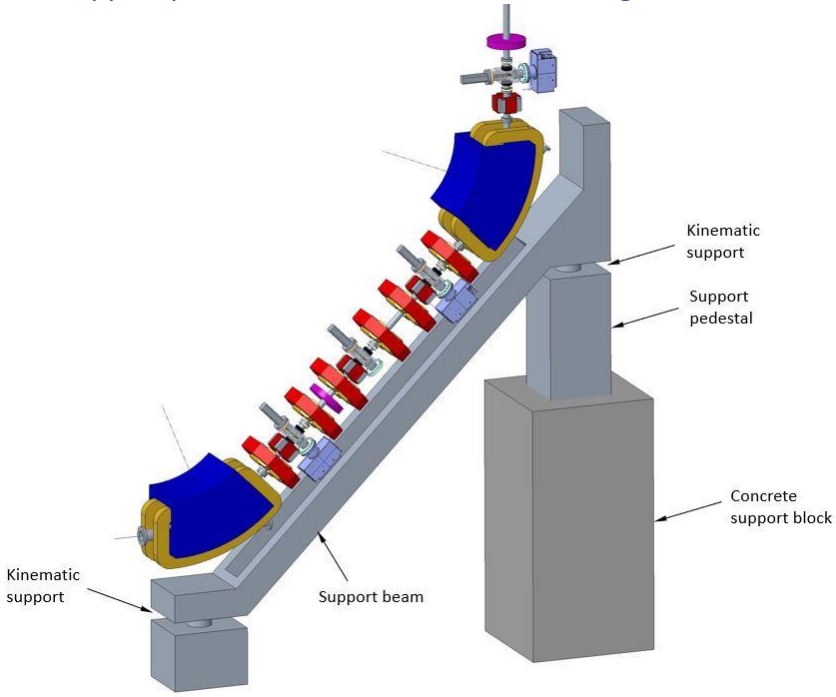

Fig 8

8. Vacuum Concepts – *Andrew Vick (STFC Daresbury)*

8.1 Introduction

The vacuum system of the LhARA project will require several different vacuum regions with a variety of operational requirements and different specifications. The first key area is the target chamber where ions are produced and there is a significant gas load. This is then directly coupled into the low energy beam line with gabor lenses, where performance needs to be optimised to avoid degrading the beam properties. The high energy line requires a similar level of vacuum to the low energy line, whereas the fixed field accelerator, due to particles recirculating, will require a higher specification of vacuum. The initial laser system will have a vacuum requirement to maintain beam quality and reduce scattering. The make-up of the end stations is currently unknown but may require a level of vacuum to be determined. Finally RF waveguide maybe needed where a vacuum system should be used over the more conventional SF_6 gas filled waveguides because of the negative environmental impact of SF_6.

The current assumed vacuum levels are presented in table 8.1 based on accelerator design experience. These values need to be confirmed by simulating gas molecule effect on beam propagation. Vacuum modelling will then be required on the mechanical design to ascertain where to place pumps to achieve these levels of vacuum.

Subsystem	Mean working pressure (mbar)
Laser systems	TBC
Laser beam Conditioning chamber	TBC
Target chamber	1×10^{-6}
Gabor lenses	1×10^{-8}
Low energy line	1×10^{-8}
Low energy in vitro end station	TBC
Fixed Field Accelerator	1×10^{-9}
High energy line	1×10^{-8}
High energy in vitro end station	TBC
High energy in vivo end station	TBC

Table 8.1 Mean working pressure for each vacuum region

The LhARA vacuum system requirements falls comfortably in the ultra-high vacuum region and therefore the general design principles for this vacuum regime will be adopted. The Vacuum Quality Assurance Documents developed at Daresbury Laboratory, for modern accelerator applications, provide a good example of design principles that can be adopted.

8.2 Vacuum Technology

In general, the vacuum system design of LhARA is based on well-tried and well understood design principles. The machine will be split into vacuum regions separated by gate valves for practical reasons and for machine protection. Dividing the machine into discrete vacuum regions makes it easier to install and commission whilst at the same time simplifying maintenance and breakdown interventions. In most circumstances gate valves will be all-metal. Roughing valves (right angled valves) and let up valves will be located in each vacuum region. ConFlatTM Flange (CF) will be used as the most common type of flange connection for ultra-high vacuum systems and uses the knife-edge principle to achieve an all-metal vacuum seal.

All vacuum components will undergo a full UHV cleaning procedure followed by a vacuum bake to 250°C for 24 hours before installation (ex-situ) where possible. This will reduce contaminants and surface outgassing enabling the design pressure to be reached. The LhARA beam line is approximately 80 m of beam pipe with a number of chambers for screen diagnostics and 7 gabor lenses. Predominately, this needs to be held at a base pressure of $1x10^{-8}$ mbar. The number of 100 l/s ion pumps required to achieve a base pressure of $9x10^{-9}$ is calculated using the vessel surface area and relevant outgassing figures. For a stainless steel vessel 80 m in length and 38 mm in diameter with 18 screen chambers, UHV cleaned and baked ex-situ a minimum of 31 ion pumps are required. Additional pumping speed will be required for the larger surface area of the gabor lenses, where we may use a higher capacity pump to achieve the vacuum level required or increase the number of pumps in this area.

Vacuum will be achieved using pumping carts, a combination of turbo-molecular pumps backed by scroll pumps, to quickly remove gas from the section. Ion pumps with optional NEG (non-evaporable getter) cartridges will then be used for maintaining vacuum during

normal operations. The ion pumps have the advantage of being static and so do not introduce any vibrations into the system. NEG cartridge pumps once activated have the ability to pump without electrical power and may be a useful addition to reduce energy demand. The laser transport lines, target chamber and differential pumping will use turbo-molecular pumps backed by scroll pumps to achieve the desired working pressures.
The vacuum system will be equipped with the relevant diagnostic instrumentation in each section, vacuum gauges (Pirani and Inverted Magnetron) and residual gas analysis. This allows the environment to be monitored, analysed and problem solving to be carried out when required. The vacuum system will be linked into the controls system for monitoring and to enable machine protection. Interlocks between sections will be used to prevent accidental venting of the machine or catastrophic failure, these will be driven by the diagnostic instrumentation.
The control system should also be enabled with a 'standby' mode allowing the controlled reduction of running pumps and controllers. In conjunction with NEG this allows the electrical power demand to be reduced impacting the CO_2 production and running costs.

8.3 Modelling

As usual, a number of iterations of machine layout and calculation of pressure distributions will be required before a satisfactory final scheme of vacuum pumping can be determined in the TDR stage. Two areas have been highlighted as challenging from a vacuum perspective and require further investigation to understand if the concept works.
The first is the vacuum connection of the target chamber to the low energy beam line due to different operating pressures of $x10^{-8}$ and $x10^{-6}$ mbar. The calculation of the conductance of the nozzle between the two will give an understanding of the impact on the vacuum from connecting these two volumes. The nozzle diameter can be optimised between ion beam diameter requirements and vacuum specification. The gas produced from the film target and its trajectory is unknown and could have an impact on the overall design due to the beaming effect.
The second challenge is the ability to pump the first gabor lens as there is a requirement to site it as close to the ion source as possible, leaving little room for a vacuum pump. As the target is a gas source we will have a higher pressure at one end of the gabor lens than the other potential detrimental to the operation of the lens. Modelling needs to be done to understand the pressure profile in this area. The mechanical design needs to be further understood in this area to enable to inclusion of pumping ports to achieve the gabor lens operating pressure.

9. Power Consumption and Cooling Requirements – *Steve Griffiths/Andy Goulden (STFC Daresbury)*

Referring to document 1272-pa1-pm-rpt-0007-v1.0-twelve-month-design-review-report (pages 73-76) the power consumption and cooling requirements are well described and have not changed significantly since the report was published.

Work is progressing in the region of the FFA combined function magnet, the power and water cooling requirements will need to be reviewed when the magnet design has been determined.

References

[1] "Ferrite cavities", H. Klingbeil (Darmstadt, GSI), CERN Yellow Report CERN-2011-007, 299-317
[2] "FFA magnet prototype for high intensity pulsed proton driver", Rodriguez, Iker et al, JACow, IPAC2023, TUPM032